IEEE Photonics Journal
An IEEE Photonics Society Publication

Numerical Analysis of Asymmetric Silicon Nanowire Waveguide as Compact Polarization Rotator

Volume 3, Number 3, June 2011

D. M. H. Leung, Member, IEEE
B. M. A. Rahman, Senior Member, IEEE
K. T. V. Grattan

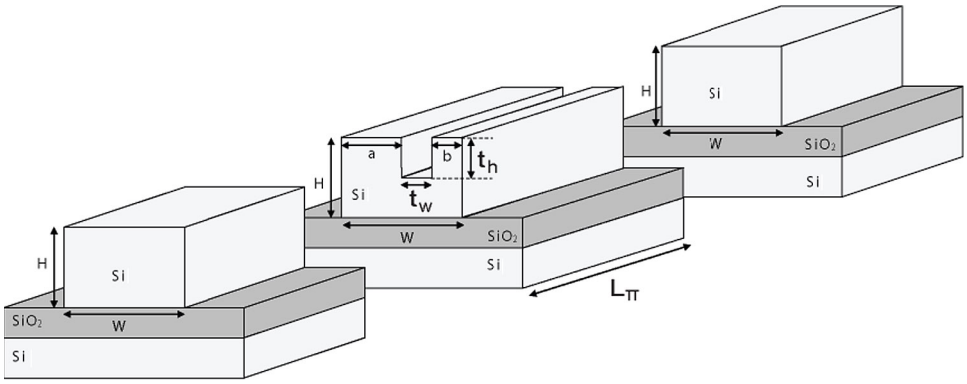

DOI: 10.1109/JPHOT.2011.2140098
1943-0655/$26.00 ©2011 IEEE

Numerical Analysis of Asymmetric Silicon Nanowire Waveguide as Compact Polarization Rotator

D. M. H. Leung, *Member, IEEE*, B. M. A. Rahman, *Senior Member, IEEE*, and K. T. V. Grattan

School of Engineering and Mathematical Sciences, City University London, EC1V 0HB, London U.K.

DOI: 10.1109/JPHOT.2011.2140098
1943-0655/$26.00 ©2011 IEEE

Manuscript received March 9, 2011; revised March 29, 2011; accepted March 29, 2011. Date of publication April 7, 2011; date of current version May 6, 2011. Corresponding author: D. M. H. Leung (e-mail: D.M.H.Leung@city.ac.uk).

Abstract: In this paper, an ultracompact design of a low-loss silicon (Si) polarization rotator based on a silicon-on-insulator platform, which contains an asymmetric strip Si nanowire waveguide core, is presented. A full-vectorial finite element method and the least squares boundary residual method are used to study the effects of the device parameters, the results of which indicate that a very high polarization conversion with a very low polarization crosstalk is possible.

Index Terms: Optical devices, optical waveguides, numerical analysis, finite element methods, numerical simulation, silicon devices, nanophotonics, polarization rotator.

1. Introduction

As the telecommunication industry embraces higher optical transmission networks, the importance of minimizing the unexpected polarization rotation and polarization crosstalk to compensate the polarization mode dispersion (PMD) [1] in an optical transmission network is of great interest in the design of polarization diversity photonics devices and photonic integrated circuits (PICs) [2]. Nowadays, PICs can improve reliability and reduce the size of complex devices by using fewer components. However, so far, there has not been a large-scale PIC that has been commercially deployed [3] because of the high development cost and poor flexibility associated with the fabrication processes of monolithically integrated subsystems. Recently, it has been suggested [4] that silicon (Si) with silicon-on-insulator technology (SOI) can be considered to be a material choice for designing and integrating dense PIC and optoelectronic integrated circuit (OEIC) devices.

Si can be chosen to build compact optical devices because it allows a high refractive index contrast for light guiding and can have comparatively low optical losses at the optical telecommunication wavelengths as well. It has already been well adapted to the complementary metal–oxide–semiconductor (CMOS) fabrication processes found in the semiconductor industry. It is also found that when building optoelectronic devices, Si is an inexpensive material to use when compared with other exotic materials such as Lithium Niobate ($LiNbO_3$), Gallium Arsenide (GaAs), and Indium Phosphide (InP). Si waveguides based on the SOI platform can also be used as building blocks in many Si PIC systems, such as nanowaveguides, compact bends, directional couplers, power splitters, ring resonators, arrayed waveguide filters, modulators, lasers, and polarization rotators. Polarization rotators and polarization splitters can be used together to design polarization diversity OEICs. In this paper, the optimization of the design of a compact Si polarization rotator based on SOI

technology is presented. This Si polarization rotator reported here has a relatively small footprint and has very low losses compared with the other polarization rotators so far reported, such as the single-section passive polarization rotator [5].

It is well known that modes in optical waveguides with 2-D confinement are hybrid in nature, with all the components of their **E** and **H**-fields being present. This modal hybridness becomes more prominent as the index contrast increases, as in an Si nanowire. For the hybrid modes in a complex OEIC system, polarization is a major issue because power can be exchanged between the polarization states in the presence of junctions, tapers, slanted sidewalls, [6], bends, or other discontinuities. Therefore, sometimes, it is necessary to have a fixed degree of polarization state, such as a transverse electric (TE) or a transverse magnetic (TM) polarization state, and it may also be necessary to rotate an incoming polarization state. It was reported that polarization rotation can be achieved by applying the electrooptic effect in $LiNbO_3$ [7] and InP [8]. However, it has also been suggested that a passive polarization converter [9] would be much preferred for use, because it would be much simpler to fabricate and to process. In particular, a passive polarization converter based on the use of asymmetrically periodic loaded rib waveguides had also been reported [10], but such a converter has a relatively large device length. To minimize the device length and to reduce the excess loss, a single-section passive polarization rotator [5] has been suggested, but it required a complicated fabrication process, often due to its tilting [11] or slanting sidewalls [12] [13]. The Si polarization rotator proposed here shows a very compact design without a slanted sidewall, requires a less complex fabrication process, and is compatible with mature CMOS technology, which is backed by the well-established semiconductor industry. However, with the index contrast being high, the modes are hybrid in nature with all the six components of the **E** and **H**-fields, which requires a full-vectorial treatment. The asymmetry of the Si nanoscale waveguide, which consists of a trench section in the Si strip core waveguide, has therefore been rigorously investigated in this work by using an **H**-field full-vectorial finite element method (FEM) [14] to calculate the propagation constant and the modal field profiles of the proposed waveguide structure, as well as an Si strip waveguide. A beam propagation method (BPM) [15] can be used to calculate the power conversion between the two polarization states; however, for the proposed structure consisting of only two discrete interfaces, the least squares boundary residual (LSBR) [16] method would be more efficient to use to find the excited modal coefficients at the butt-coupled junctions, as well as to find the resulting polarization rotation. The half-beat length and polarization crosstalk, along with the power loss in the polarization rotator, are presented. Finally, different lateral offsets between the butt-coupled sections are also considered to further improve the design.

2. Theory

The accurate calculation of the magnitudes of the nondominant field components and their profiles for the fundamental quasi-TE and TM polarized modes are of great importance when designing a polarization rotator. In the design of a compact optical polarization rotator, a full-vectorial FEM is used to obtain the modal field profiles of the constituent waveguides. The full-vectorial FEM is used because the modes in optical waveguide with a very strong index contrast are hybrid in nature. In this formulation, all the **H**-field components are continuous across the dielectric interface. On the other hand, since the normal component of the **E**-field is discontinuous around the interface, an equivalent **E**-field based approach would be less satisfactory. As for the hybrid modes, a significant nondominant field component exists around the dielectric interfaces, and hence, the **H**-field formulation can be used to treat such waveguides more rigorously. In the design process, it is necessary not only to increase the magnitude of the nondominant field components but its profile can be optimized to enhance its overlap with the dominant field components to achieve the maximum polarization rotation as well. The full-vectorial formulation used here is based on the minimization of the following energy functional [14] in terms of the nodal values of the full **H**-field vector:

$$\omega^2 = \frac{\int \left[(\nabla \times \mathrm{H})^* \cdot \varepsilon^{-1} (\nabla \times \mathrm{H}) + p(\nabla \cdot \mathrm{H})^* (\nabla \cdot \mathrm{H}) \right] dxdy}{\int \mathrm{H}^* \cdot \ \mu \mathrm{H}\, dx\, dy} \tag{1}$$

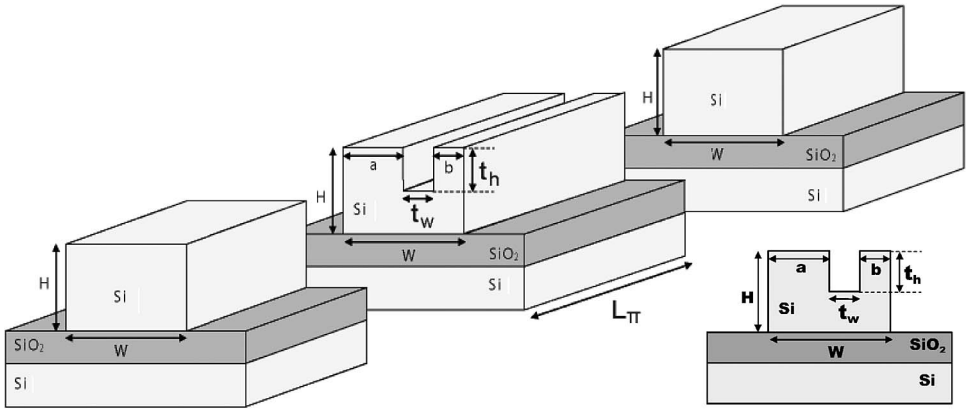

Fig. 1. Schematic diagram of the asymmetric polarization rotator butt-coupled to input and output of a SOI strip waveguide, and a cross section of the Si asymmetric strip rotator.

where **H** is the full-vectorial magnetic field; * denotes a complex conjugate and transpose; ω^2 is the eigenvalue, where ω is the angular frequency of the wave; and ε and μ are the permittivity and permeability, respectively. The penalty function approach has also been incorporated to impose divergence-free condition of the magnetic field to reduce the appearance of spurious modes and *p* is the dimensionless penalty parameter. This full-vectorial FEM modal solution is also used to determine the polarization beat length between the quasi-TE and TM polarized fundamental modes.

A junction analysis approach is also used, as the proposed polarization rotator structure is composed of two butt-coupled uniform waveguide sections with only two discrete interfaces between them. A powerful numerical approach, i.e., the LSBR method [16], has been used, which rigorously satisfies the continuity of the tangential electric and magnetic fields at the junction interface in a least squares sense, and the modal coefficients of the transmitted and reflected modes at the discontinuity interface can be obtained. The LSBR method is used to look for a stationary solution to satisfy the continuity conditions by minimizing the error energy functional **J**, as given by [16]

$$J = \int_{\Omega} \left|E_t^I - E_t^{II}\right|^2 + \alpha \cdot Z_0^2 \left|H_t^I - H_t^{II}\right|^2 d\Omega \tag{2}$$

where Z_0 is the free-space impedance, and α is the dimensionless weighting factor to balance the electric and magnetic components of the error functional **J**. The integration is carried out over the junction interface Ω between the straight and the asymmetric Si waveguides.

3. Results

Fig. 1 shows the single-stage polarization rotator, which consists of two Si strip waveguides with straight sidewalls, where both are butt coupled to an Si asymmetric strip polarization rotator waveguide in the middle. In the design of a polarization rotator, an asymmetric section which supports the highly hybrid modes is sandwiched between two standard Si waveguides where the hybridness is small. When a quasi-TE (or quasi-TM) mode from a standard Si waveguide with its polarization angle at nearly zero degrees (or indeed 90°) is launched into the asymmetric section (which supports highly hybrid modes with polarization direction $\pm 45°$), then both of them are excited almost equally to satisfy the continuity of the $\mathbf{E_t}$ and $\mathbf{H_t}$ fields at that interface. These two highly hybrid modes travel along the asymmetric sections. The half-beat length is a key parameter used in order to identify the optimum length of this asymmetrical section to achieve the maximum polarization rotation. The half-beat length is defined as $L_\pi = \pi/\Delta\beta$, where $\Delta\beta$ is the difference between the propagation constants of the H_{11}^y and the H_{11}^x modes. After propagating a distance $L = L_\pi$, the original phase condition between the highly polarized modes would be reversed, and

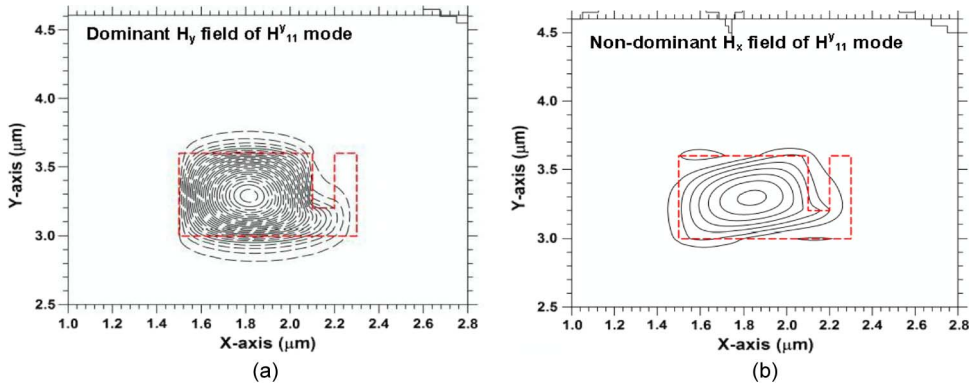

Fig. 2. Contour plots of (a) the dominant H_y field profile and (b) the nondominant H_x field profile of the H^y_{11} mode with $W = 800$ nm and $H = 600$ nm, $t_w = 100$ nm and $t_h = 400$ nm.

the polarization state of the superimposed modes would be rotated by 90°. If a standard Si waveguide (with smaller modal hybridness) is placed at this position, this quasi-TM (or quasi-TE) mode would propagate without any further polarization rotation.

The structure under consideration is an Si asymmetric strip polarization rotator waveguide; the cross section of this typical waveguide is also shown in Fig. 1 as an inset. This particular waveguide structure consists of a single trench in the waveguide core and such a waveguide can easily be fabricated by using a SOI wafer on an Si substrate. A single-trench photoresist mask can be used on the surface of the Si core and then etched down to the desire depth in the Si core waveguide. The Si core waveguide then either can be buried under a thick silica (SiO_2) or covered by air or other polymers. In the numerical simulations used, the structure is surrounded by air, and initially, the width W is varied in order to study its effect on modal field profiles and, particularly, the effect of polarization degeneration. In this analysis, the operating wavelength is considered to be 1.55 μm, and at this wavelength, the refractive index of the Si core is taken as 3.5, and that of the SiO_2 cladding and the SiO_2 buffer layer is taken as 1.5. The thickness of the Si core waveguide H is taken as 600 nm, and that of the lower SiO_2 buffer layer is taken as 1.50 μm. If a lesser height is considered for the Si layer, then the width required to bring polarization degeneration would have been also smaller and such that the waveguide would be very considerably lossy. Hence, in this study, a greater height is deliberately considered. The thickness t_h and the width t_w of the trench waveguide section and the width, "a" of the rotator waveguide section are varied to optimize the design, while the width "b" of the rotator waveguide section is taken to be 100 nm.

A full-vectorial FEM is used in this study to obtain the modal solutions of the single-trench Si waveguide. In this analysis, more than 20 000 first-order triangular elements have been employed to represent the waveguide structure. In this particular waveguide, for the quasi-TE (H^y_{11}) mode, the H_y field component is dominant, and H_x and H_z are the nondominant components. Similarly, H_x is the dominant field component of the quasi-TM (H^x_{11}) mode. The spatial profile of the dominant H_y field component of the quasi-TE mode is shown in Fig. 2(a) for a larger guide width $W = 800$ nm. In this case, the width, t_w, of the single-trench structure is taken as 100 nm, and the height t_h is taken as 400 nm, and the overall Si core waveguide is surrounded with air, but if necessary, other materials, such as SiO_2 or polymer, can also be considered. In this case, the modal hybridness was relatively small, and the H_y field profile shows that the maximum optical intensity occurs near the geometrical-center of the larger Si core region. However, due to the asymmetry of the waveguide, the field profile is slightly asymmetric, and it shows that the field extends more to the lower SiO_2 substrate region, as well as by a smaller amount into the air region. The effective index n_e of the H^y_{11} mode was found to be 3.11085. The nondominant H_x field component of the quasi-TE mode is shown in Fig. 2(b), and it can be observed that this field profile is nearly a similar shape to that of the dominant H_y field profile. In this case, the maximum magnitude of the H_x field profile is found to be about 25% of the maximum value of the dominant H_y field. It should be noted that the nondominant

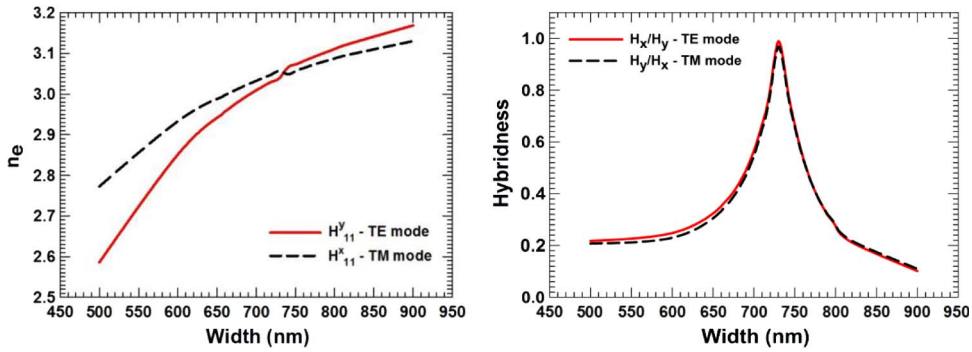

Fig. 3. Variations of (a) effective index n_e and (b) the hybridness, with the width *W* for the fundamental TE and TM modes.

H_x field profile for a Si strip without the trench section has a very small magnitude with the odd-like symmetry along the *y*-axis, but this is not shown here.

It is important, however, in the design of a polarization rotator, to enhance the modal hybridness of the asymmetric structure further. In Fig. 3(a), the variations of the effective index (n_e), with the width (W) for the fundamental quasi-TE (H_{11}^y) and TM (H_{11}^x) modes, are presented for the air cladding structure. In this case, as the width W is reduced, and both t_w and *b* were kept constant at 100 nm. It can be observed that when the width of the waveguide is large, n_e is closer to the refractive index of the Si. As *W* decreases, n_e also decreases and gets closer to the refractive index of SiO_2, where a mode reaches its cutoff. However, it is shown here that the effective index of the H_{11}^y mode crosses that of the H_{11}^x mode at a width *W* lying between 730 nm and 740 nm, when the equivalent width is comparable to its height, and these two polarized modes become degenerate. In fact, their effective index values do not actually cross each other, but the modes rather transform from one dominant polarization state to the other in this region.

The effect of the waveguide width *W* on the modal hybridness is shown in Fig. 3(b). The modal hybridness is defined as the ratio of the maximum value of nondominant field to that of the dominant field. In the case of the H_{11}^y mode, the modal hybridness is given by the ratio of the nondominant H_x field (the maximum value) to the dominant H_y field (its maximum value), and it is shown here by a solid line. The modal hybridness of the H_{11}^x mode, calculated from the ratio of the maximum value of the H_y field to its H_x field, is also shown as a dashed line. It can be seen here that for both polarized modes, when *W* is reduced from 900 nm to 730 nm, the hybridness is increased. At a width equal to 730 nm, their hybridness values reach their maximum of about one, in which it indicates that both of the transverse field components are identical. Under this condition, the polarization directions are $\pm 45^\circ$ with respect to the x and y-axes for the two polarized modes. For both the polarized modes, it is also shown that as *W* reduces further, the hybridness decreases. The modal hybridness of the H_{11}^x mode also follows a similar trend to that of the H_{11}^y mode, and its maximum hybridness also occurs at a width of 730 nm.

The half-beat length is a key parameter used in order to identify the optimum length of the asymmetrical section to achieve the maximum polarization rotation. At the half-beat length, the phase mismatch between the two polarized modes H_{11}^y and H_{11}^x, is also at its minimum. Fig. 4(a) shows the variations of the half-beat length with the width. Therefore, in this study, when the two modes are degenerate, their hybridness is 1.0, their polarization angles are $\pm 45^\circ$, and the half-beat length, L_π also reaches the maximum value of 48 μm. Hence, the length of the central asymmetric section with the trench needs to be 48 μm, which is reasonably short, compared with other designs reported so far [17], [18].

As mentioned before, the incoming TE (or TM) x- (or y-) polarized wave of a standard guide would excite two highly hybrid $\pm 45^\circ$ polarized modes in the asymmetric section. To quantify further in the analysis, the scattering coefficients at the junction need to be obtained. In this study, a rigorous

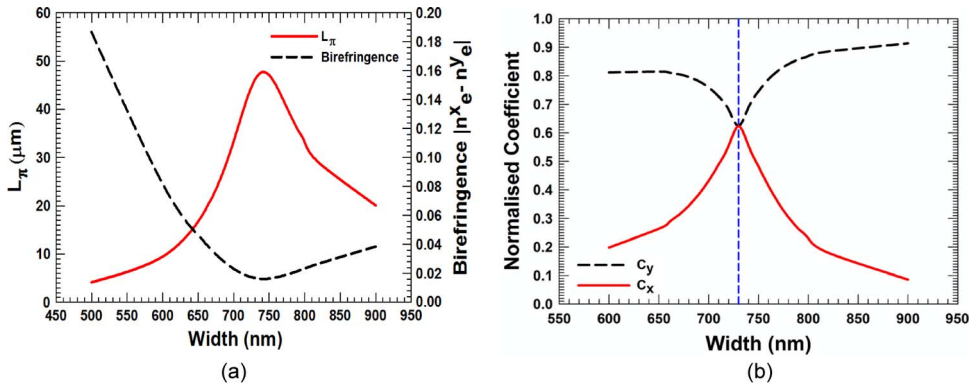

Fig. 4. Variations of (a) half-beat length L_π and birefringence and (b) the transmitted modal coefficients C_x and C_y, with the width W for the fundamental TE mode.

numerical approach using the LSBR has been employed to obtain the modal coefficients at the discontinuity interface by enforcing the boundary conditions in a least squares sense. In this example, the H^y_{11} mode of the vertical sidewall waveguide (without the trench section), where the modal hybridness is very small (but it was not neglected), is launched into the single-trench waveguide section, which excites two highly hybrid modes to satisfy the necessary boundary conditions. The transmitted modal coefficients, i.e., C_y and C_x of the H^y_{11} and H^x_{11} modes, respectively, were calculated, and their variations of these two modal coefficients with the single-trench waveguide width W are shown in Fig. 4(b). It can be seen that as W reduces, the modal coefficient of the transmitted H^x_{11} polarized fundamental mode C_x reaches a maximum value of 0.6236 at $W = 730$ nm and then reduces to 0.198 at $W = 600$ nm. It is also shown that the modal coefficient of the transmitted quasi-TE polarized fundamental mode, C_y, reaches its minimum value of 0.6234 as W reduces to 730 nm. For a system where 100% polarization rotation can be achieved without any power loss, these two values are expected to be equal to $1/\sqrt{2}$, indicating that each mode is carrying equal and half of the total power. Hence, in this case, at the mode degeneracy condition, since the modal coefficient of both the modes are similar, the power carried by each of them is also similar, and here, the total power loss is found to be only 1.09 dB, which is very small. Reflections from both the butt-coupled interfaces were small, with the reflection coefficient less than 2%.

As these two polarized modes travel along the single-trench section waveguide, the polarization states of these two modes will be continuously rotated due to the phase difference between them. From the modal coefficients and their full-vectorial field profiles, the polarization conversion can be calculated. At a distance L_π, the polarization state will be fully rotated, i.e., an incident TE mode will transform to a TM mode, and this can be further guided unchanged in a butt-coupled standard Si waveguide with vertical sidewalls. The variations of the polarization conversion with the width W is shown in Fig. 5. It can be clearly seen that as W increases from 600 nm, the normalized power conversion of TE (P_y) to TM (P_x) reaches a maximum value of 0.9947 at $W = 730$ nm and then reduces as W increases further. With ± 10 nm tolerance from the maximum power conversion at the optimum width, the power conversion is found to be 0.9467 when $W = 720$ nm and 0.9557 when $W = 740$ nm, which shows that the polarization conversion only decreases by about 5% for a derivation of ± 10 nm from the desired optimum width. Along the polarization rotator, the power P_y of the TE polarized mode is incident at the junction between two interfaces, and most of the power will be converted into TM polarized mode P_x at the end of this section. However, there may remain some power from P_y; here, this normalized residual power P_y is referred to as crosstalk. In this study, the crosstalk is defined as the unwanted polarized power (in this case P_y), normalized to the total input power, which remains at the end of the single-trench waveguide. It is again shown here that at this 730 nm optimum width, the crosstalk reaches a minimum value of -22.82 dB, which a very low value. However, with ± 10 nm derivation from the optimum width, the crosstalk values are -13.54 dB and -12.73 dB when the widths are at 740 nm and 720 nm, respectively. The half-beat

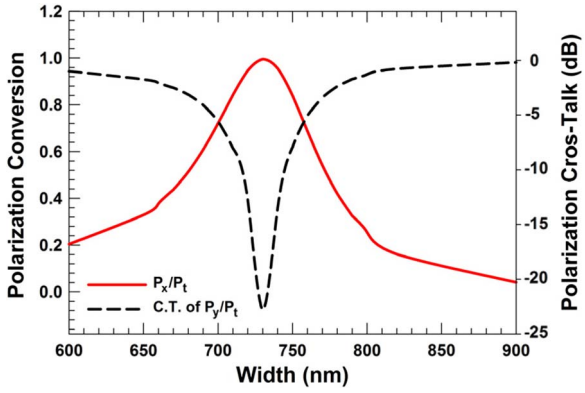

Fig. 5. Variations of the polarization conversion and the polarization crosstalk.

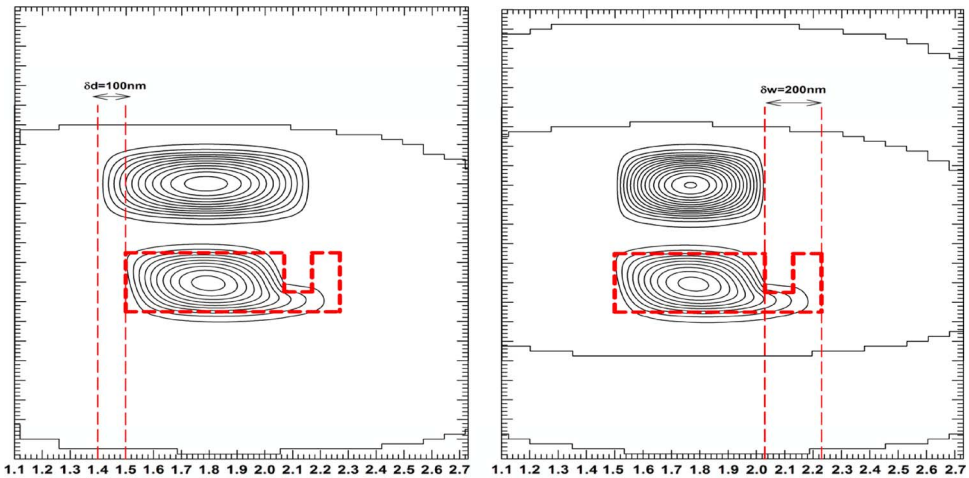

Fig. 6. Performance of the straight-to-polarization rotator coupled waveguide with two different offsets. (a) $\Delta x = 100$ nm. (b) $\Delta w = 200$ nm.

length and the modal hybridness also depend on the operating wavelength. When the operating length is changed to 1450 nm, the resulting modal hybridness, half-beat length, polarization conversion, and polarization crosstalk are 0.94, 54 μm, 94%, and -11.83 dB, respectively and for the operating wavelength of 1650 nm, these values were 0.92, 39 μm, 92%, and -10.80 dB, respectively.

It was evident that the spatial field profiles of the straight section waveguide and the single-trench polarization rotator waveguide are different; in particular, the field profile of the single-trench polarization rotator had a smaller width and was off-center due to the presence of the trench. It has often been assumed by others (and in the above section) that the input strip waveguide is of the same width as that of the polarization rotator waveguide section and that their two vertical end sidewalls are exactly aligned. However, it does not need to be this way; rather, by employing an offset, the fields in both sides of the junction can be matched even better. Therefore, the different lateral shifts between the guides are introduced to study the effect on the polarization rotation, as well as on the insertion loss. To do so, first, an offset is introduced where the input straight sidewall waveguide is shifted to the left when coupling to the single-trench waveguide to enhance the field matching. In this example, the width of the waveguide is taken as 770 nm, the offset Δx is taken as 100 nm, and it is shown in Fig. 6(a) how this offset can be introduced. It can be observed that the

location of the field maximum of the straight waveguide is now better aligned with that of the single-trench waveguide when the offset is introduced. In this case, the transmitted modal coefficients of the H_{11}^{y} and H_{11}^{x} modes were found to be 0.703 and 0.634, respectively, which yield 98.47% conversion with the polarization crosstalk value slightly deteriorated to reach a value of around -18.16 dB. However, the loss in this case was found to be 0.47 dB, which represents a reduction of almost 50% in the power loss, when compared with the original design without the offset.

An alternative offset method has also been studied, where the width of the input straight sidewall waveguide is reduced to improve the mode matching. Fig. 6(b) shows how this particular offset can be achieved. The width of the straight sidewall waveguide is reduced by Δw, with the single-trench waveguide width kept at 730 nm. It can be observed in Fig. 6(b) that although the straight sidewall is reduced by 200 nm to 530 nm, overall, their field profiles match much better. Using the LSBR method, the transmitted modal coefficients of the H_{11}^{y} and H_{11}^{x} modes were found to be 0.698 and 0.681, respectively. The maximum polarization conversion of the TE to TM was found to be 99.42% (again, a very high value), but the loss was found to be only 0.21 dB, which a significantly smaller value when compared with the loss without the offset and with equal width at 730 nm. The crosstalk in this case was also found to be similar to the value of crosstalk when no lateral offset was applied, with its value at -22.38 dB.

4. Conclusion

In this paper, a compact polarization rotator based on an asymmetric Si nanowire has been presented. The rigorous full-vectorial FEM was used to characterize such structures with very strong modal hybridness. Such a compact asymmetric waveguide with its vertical sidewall is easy to fabricate when compared with the other asymmetric polarization rotators with slanting sidewalls. It was found that more than 99% of polarization conversion can be obtained for a device length of 48 μm in such a design. It is also shown that the total power loss is only 0.21 dB by optimizing the offset between the sections. In this case, slightly larger Si dimensions are considered to reduce the propagation loss near the degeneration point, as well as to avoid a slot mode when a 100-nm slot is introduced. However, more specific system requirements may be obtained and optimized, including the effects of fabrication tolerances, as required.

Acknowledgment

The authors wish to thank the anonymous reviewers for their valuable suggestions.

References

[1] J. L. Liu, Y. Shi, F. Wang, Y. Lu, S. L. Gu, R. Zhang, and Y. D. Zheng, "Study of dry oxidation of triangle-shaped silicon nanostructure," *Appl. Phys. Lett.*, vol. 69, no. 12, pp. 1761–1763, Sep. 1996.

[2] U. Hilbk, T. Hermes, P. Meissner, C. Jacumeit, R. Stentel, and G. Unterborsch, "First system experiments with a monolithically integrated tunable polarization diversity heterodyne receiver OEIC on InP," *IEEE Photon. Technol. Lett.*, vol. 7, no. 1, pp. 129–131, Jan. 1995.

[3] S. J. B. Yoo, "Future prospects of silicon photonics in next generation communication and computing systems," *Electron. Lett.*, vol. 45, no. 12, pp. 584–588, Jun. 2009.

[4] M. Lipson, "Guiding, modulating, and emitting light on silicon-challenges and opportunities," *J. Lightw. Technol.*, vol. 23, no. 12, pp. 4222–4238, Dec. 2005.

[5] B. E. Little and S. T. Chu, "Theory of polarization rotation and conversion in vertically coupled microresonators," *IEEE Photon. Technol. Lett.*, vol. 12, no. 4, pp. 401–403, Apr. 2000.

[6] N. Somasiri, B. M. A. Rahman, and S. S. A. Obayya, "Fabrication tolerance study of a compact passive polarization rotator," *J. Lightw. Technol.*, vol. 20, no. 4, pp. 751–757, Apr. 2002.

[7] R. C. Alferness and L. L. Buhl, "High-speed waveguide electro-optic polarization modulator," *Opt. Lett.*, vol. 7, no. 10, pp. 500–502, Oct. 1982.

[8] M. Schlak, C. M. Weinert, P. Albrecht, and H. P. Nolting, "Tunable TE/TM-mode converter on (001)-InP-substrate," *IEEE Photon. Technol. Lett.*, vol. 3, no. 1, pp. 15–16, Jan. 1991.

[9] K. Mertens, B. Scholl, and H. J. Schmitt, "Strong polarization conversion in periodically loaded strip waveguides," *IEEE Photon. Technol. Lett.*, vol. 10, no. 8, pp. 1133–1135, Aug. 1998.

[10] Y. Shani, R. Alferness, T. Koch, U. Koren, B. I. Miller, and M. G. Young, "Polarization rotation in asymmetric periodic loaded rib waveguides," *Appl. Phys. Lett.*, vol. 59, no. 11, pp. 1278–1280, Sep. 1991.

[11] H. Deng, D. O. Yevick, C. Brooks, and P. E. Jessop, "Design rules for slanted-angle polarization rotators," *J. Lightw. Technol.*, vol. 23, no. 1, pp. 432–445, Jan. 2005.
[12] B. M. A. Rahman, S. S. A. Obayya, N. Somasiri, M. Rajarajan, K. T. V. Grattan, and H. A. El-Mikathi, "Design and characterization of compact single-section passive polarization rotator," *J. Lightw. Technol.*, vol. 19, no. 4, pp. 512–519, Apr. 2001.
[13] C. Brooks, P. E. Jessop, H. Deng, D. O. Yevick, and G. Tarr, "Passive silicon-on-insulator polarization-rotating waveguides," *Opt. Eng.*, vol. 45, no. 4, p. 044603, Apr. 2006.
[14] B. M. A. Rahman and J. B. Davies, "Finite element solution of integrated optical waveguides," *J. Lightw. Technol.*, vol. 2, no. 5, pp. 682–688, Oct. 1984.
[15] S. S. A. Obayya, B. M. A. Rahman, and H. A. El-Mikati, "New full-vectorial numerically efficient propagation algorithm based on the finite element method," *J. Lightw. Technol.*, vol. 18, no. 3, pp. 409–415, Mar. 2000.
[16] B. M. A. Rahman and J. B. Davies, "Analysis of optical waveguide discontinuities," *J. Lightw. Technol.*, vol. 6, no. 1, pp. 52–57, Jan. 1988.
[17] S. H. Kim, R. Takei, Y. Shoji, and T. Mizumoto, "Single-trench waveguide TE-TM mode converter," *Opt. Express*, vol. 17, no. 14, pp. 11 267–11 273, Jul. 2009.
[18] H. Deng, D. O. Yevick, C. Brooks, and P. E. Jessop, "Fabrication tolerance of asymmetric silicon-on-insulator polarization rotators," *J. Opt. Soc. Amer. A, Opt. Image Sci.*, vol. 23, no. 7, pp. 1741–1745, Jul. 2006.